Range Migration Compensation Based on Range-Direction Coupling in SFDLFM MIMO radar

LI JUN, LIU HONGMING, HE ZISHU, CHENG TING
School of Electronic Engineer
University of Electronic Science and Technology of China
Jianshe North Road Sec.2 No.4 (610054)
CHENG DU, CHINA
lijun_sc@hotmail.com, kjlhm@163.com, zshe@uestc.edu.cn, citrus@uestc.edu.cn

Abstract: - Wide low-gain transmitting beam and long time integration are adopted in the orthogonal signal MIMO radar to survey the interested area. The range migration of moving target is a pivotal problem faced in the MIMO radar. Orthogonal LFM signal is one of the most familiar waveforms in MIMO radar, and this paper discusses the range migration compensation problem in the MIMO radar using Stepped Frequency Division Linear Frequency Modulation (SFDLFM) signal. A new compensation method based on the proper range-direction coupling relationship is put forward. It can achieve a good compensation effect with low computation complexity. Theoretical deduction and simulation results demonstrate the validity of this method.

Key-Words: - MIMO radar, range migration, coherent integration, motion compensation, SFDLFM signal, range-direction coupling

1 Introduction

As orthogonal signal MIMO radar[1]~[4] adopts wide low-gain transmitting beam, it is required much longer integration time to obtain enough SNR. To offset the loss of long-time integration, range migration compensation is necessary for the detection of moving targets. Many researches have been done on motion compensation containing range migration compensation[5]~[10], where the basic approaches include range-bin realignment[5], envelope interpolation algorithm[7], Keystone transform[9][10], etc.

The signal processing of MIMO radar becomes more complex because of using orthogonal waveforms, and the factors affecting the envelope position gets to be manifold. Therefore, the approach of range migration compensation may be more flexible. The Synthetic Impulse and Aperture Radar (SIAR)[11]~[13] is the rudiment of orthogonal signal MIMO radar, and the long time coherent integration problem of SIAR is studied in reference [14]. However, the adopted method of motion compensation is ordinary means. The computation burden and the processing complexity problems will restrict the application of traditional methods in MIMO radar. More practical method with little additional computation load is required to resolve long time coherent integration problem.

Orthogonal LFM signals are one of the most familiar waveforms in MIMO radar. For the simplicity of generation and processing, linear frequency modulation (LFM) signal has attracted much attention of radar designer. In order to increase the single pulse energy while maintaining high range resolution, large time-width LFM signal is commonly used in conventional radar. LFM signal is also a key signal form for the research of SIAR and MIMO radar. In reference [15], a method of realizing the high range resolution of MIMO radar using the FDLFM signal is given. In reference [16], the synthetic characteristic of MIMO radar with Stepped Frequency Division Linear Frequency Modulation (SFDLFM) signal is discussed systematically, which includes the characteristics of range-Doppler-direction coupling of the synthetical output and that of side-lobes in different conditions. The Doppler-range coupling is related to the characteristic of ambiguity function of LFM signal. The range-direction coupling is remarked in [17] and [18].

This paper discusses the range migration compensation problem in the MIMO radar using SFDLFM signal. A new method to compensate the envelope migration of moving targets is put forward. It utilizes the proper range-direction coupling relationship of the synthetical output of SFDLFM signal, and combines the compensation operation with the processing of signal synthesizing, which

greatly reduces the additional computation burden arising from the compensation processing. Therefore, it is a practical method with low complexity.

The paper is organized as follows: The echo signal model of SFDLFM MIMO radar from a moving target is given in section II. Section III analyzes the characteristic of the synthetical signal of a single period. In section IV, the main factors affecting envelope migration are discussed. Section V presents the method of range migration compensation utilizing the range-direction coupling relationship. The simulation results are given in Section VI, and Section VII concludes the whole paper.

When using SFDLFM signals, the time-domain characteristic of the synthetical signal depends mainly on the frequency arrangement characteristics and the initial phase of the transmitting array signals, which is independent of the receiving beamforming. For analyzing simplicity, it is assumed that there is only one nondirectional receiving element in the following discussion. Meanwhile, suppose the velocity of the target is constant during the coherent processing interval (CPI).

2 Signal model of the SFDLFM MIMO radar

Each of the elements of orthogonal MIMO radar radiates a unique and orthogonal waveform. The emitted signals can not be combined to form a single focused beam, instead, the radiated energy will cover a broad angular sector. Due to the reduction of transmitting gain, in order to obtain enough detection signal noise ratio (SNR), more transmitting pulses in a CPI must be required to get a long integration time.

For the simplicity of generation and processing, LFM signal is the one of the most common used waveform in modern radars. In this section, the signal model based on SFDLFM pulse trains in MIMO radar is analyzed.

Assume that the transmitting array is a uniform linear array with K elements, the signal frequencies on them are arranged by a stepped sequence. Denote the frequency assigned to the k -th element as $f_k = f_c + kf_\Delta$, $k = 0,1,\cdots,K-1$. f_c is the RF frequency of the first transmitted sub-waveform and f_Δ is the frequency interval between adjacent sub-waveforms. The frequency-time relation of each sub-waveform in SFDLFM MIMO radar is illustrated in Fig.1.

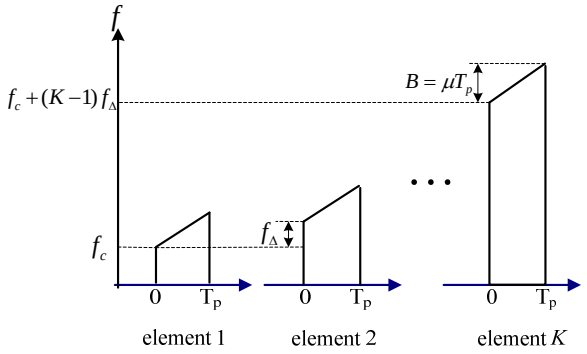

Fig.1 Frequency-time relation of each waveform in SFDLFM MIMO radar

Each element transmits a LFM pulse train with the length of M and the pulse repetition period of T (namely pulse repetition interval - PRI). The transmitted signal of the k -th element can be expressed as:

$$s_k(t) = \sum_{m=0}^{M-1} U(t - mT) e^{j2\pi(f_c + kf_\Delta)t} e^{j\phi_k} \qquad (1)$$

Where ϕ_k is the initial phase, and

$$U(t) = rect(\frac{t}{T_P}) e^{j\frac{1}{2}\mu t^2} \qquad (2)$$

is the complex modulation envelope. T_p is the pulse width, μ is the frequency modulation slope, and $rect(t/T_p)$ is the rectangular function:

$$rect(\frac{t}{T_p}) = \begin{cases} 1 & 0 \le t \le T_p \\ 0 & \text{else} \end{cases} \qquad (3)$$

In order to satisfy the orthogonality requirement, there is

$$f_\Delta T_p = N \qquad (4)$$

where N is positive integer. The sub-bandwidth of each LFM waveform is

$$B = \mu T_p \qquad (5)$$

and so the total bandwidth occupied by the transmitted signals is

$$B_{\Sigma} = B + (K-1) f_{\Delta} \quad (6)$$

where f_{Δ} may be less than B, that is the band of each transmitting channel may be partly overlapped.

The effect of target motion on the radar electromagnetic wave presents time scale changing of the returned signal (time stretching or shrinking)[19]. When the above SFDLFM signal has been transmitted by the transmitter array and reflected by a moving target, the returned signal on the receiver can be written as:

$$s_{rk}(t) = \eta_0 \sum_{m=0}^{M-1} U(\kappa(t-t_0) - mT) e^{j2\pi(f_c + kf_{\Delta})(\kappa(t-t_0))} e^{j\phi_k} e^{-jk\varphi_t} \quad (7)$$

where $\kappa = (c+v)/(c-v)$ is the compression coefficient related to the target velocity v, and c is the velocity of light. t_0 is the propagation delay of the returned signal, η_0 is the total loss factor, and φ_t is the space phase difference of the transmitting array corresponding to the direction of the target.

$$\varphi_t = 2\pi d \sin\theta / \lambda \quad (8)$$

where d is the element spacing, λ is the wavelength.

After mixing with the local oscillator signal, the obtained baseband signal is:

$$\begin{aligned} s_{rkI}(t) &= s_{rk}(t) e^{-j2\pi f_c t} \\ &= \eta_0 \sum_{m=0}^{M-1} U(\kappa(t-t_0) - mT) e^{j2\pi f_c \kappa_v t} e^{j2\pi k f_{\Delta} \kappa t} e^{-j2\pi(f_c + kf_{\Delta})\kappa t_0} e^{j\phi_k} e^{-jk\varphi_t} \end{aligned} \quad (9)$$

where $\kappa_v = \kappa - 1$.

Based on the hypothesis of narrow band signal, the compression effect on the single envelope due to the target motion can be neglected, and it is just needed to pay attention to the migration of the envelope, then we have:

$$\begin{aligned} &U(\kappa(t-t_0) - mT) = U(\kappa[(t-t_0) - mT/\kappa]) \\ &\approx U(t - t_0 - mT/\kappa) = U(t - t_0 - mT - \kappa_w mT) \end{aligned} \quad (10)$$

where $\kappa_w = 1/\kappa - 1$.

Denote t as $t = \hat{t} + mT$, where $\hat{t}$ is the "fast time" in a PRI, $\hat{t} \in [0, T]$, and m denotes the "slow time" for different period. Then, through formula (9) and (10), the base band signal $s_{rkI}(t)$ can be expressed as a bidimensional form:

$$\begin{aligned} s_{rkI}(m, \hat{t}) = \eta_0 U(\hat{t} - t_0 - \kappa_w mT) e^{j2\pi f_c \kappa_v (\hat{t} + mT)} \cdot \\ e^{j2\pi k f_{\Delta} \kappa (\hat{t} + mT)} e^{-j2\pi(f_c + kf_{\Delta})\kappa t_0} e^{j\phi_k} e^{-jk\varphi_t} \end{aligned} \quad (11)$$

So, the video signal of the receiving element can be expressed as:

$$s_{rI}(m, \hat{t}) = \sum_{k=0}^{K-1} s_{rkI}(m, \hat{t}) \quad (12)$$

In addition, we supposed that $t_0 \in [0, T]$. If this hypothesis isn't satisfied, a simple variable transform can be done.

3 Characteristic of the synthetical signal of a single period

The characteristic of the synthetical output in one period (PRI) will be discussed in this section.

The receiver processing is illustrated in Fig.2[1][20]. The returned signal is processed through a bank of matched filters to separate the components corresponding to each transmitted waveform. The matched filtering outputs are phased and combined to form an equivalent transmitting beam, and then the obtained synthetical output can be further processed by integration.

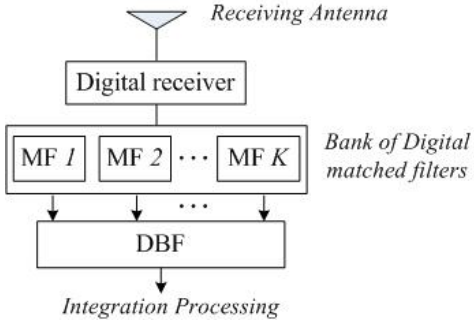

Fig.2 Matched filtering and DBF processing for received signal

The matching signal used in the matched filters can be wrote as:

$$v_g(\hat{t}) = U(\hat{t}) e^{j2\pi g f_{\Delta} \hat{t}} e^{j\phi_g} \quad g \in [0, K-1] \quad (13)$$

After matched filtering, K outputs can be obtained. Then equivalent transmitting beamforming can be done by summating the phase-shifted outputs.

Suppose the rectifying phase difference adopted in the beamforming is φ_{t_0}, then the synthetical output signal can be expressed by

$$u_c(m,\hat{t}) = \sum_{g=0}^{K-1}[\sum_{k=0}^{K-1} s_{rkI}(m,\hat{t}) \otimes v_g^*(\hat{t})]e^{jg\varphi_{t_0}} \quad (14)$$

where $\otimes$ denotes convolution operation, $*$ means conjugate operation. There are $K \times K$ components in $u_c(m,\hat{t})$ of formula (14), and one of them can be written as:

$$y_{k,g}(m,\hat{t}) = s_{rkI}(m,\hat{t}) \otimes v_g^*(\hat{t}) \quad (15)$$

$y_{k,g}(m,\hat{t})$ denotes the correlation function of the g-th transmitted signal and the k-th returned sub-waveform. Obviously, the characteristic of the synthetical signal $u_c(m,\hat{t})$ mainly depends on K components of $g=k$, namely auto-correlation functions. So

$$u_c(m,\hat{t}) \approx \sum_{k=0}^{K-1} y_{k,k}(m,\hat{t})e^{jk\varphi_{t_0}} \quad (16)$$

By means of the ambiguity function expressions of LFM signal, and let $\xi_d = kf_\Delta\kappa_v + f_c\kappa_v$, we get:

$$y_{k,k}(m,\hat{t}) = \eta_0 e^{-j2\pi f_c\kappa t_0} e^{j2\pi f_c\kappa_v mT} e^{j\frac{\mu}{2}(\hat{t}-t_0-\kappa_w mT)T_p} e^{j\pi f_c\kappa_v(\hat{t}+t_0+\kappa_w mT+T_p)} \cdot e^{jk[\pi f_\Delta(\kappa+1)\hat{t}-\pi f_\Delta(\kappa+1)t_0+\pi f_\Delta(2\kappa+\kappa_v\kappa_w)mT+\pi f_\Delta\kappa_v T_p-\varphi_t]} \cdot sac(m,\hat{t}) \quad (17)$$

Here,

$$sac(m,\hat{t}) = \begin{cases} \dfrac{2\sin((\mu(\hat{t}-t_0-\kappa_w mT)+2\pi\xi_d)\frac{T_p-|\hat{t}-t_0-\kappa_w mT|}{2})}{\mu(\hat{t}-t_0-\kappa_w mT)+2\pi\xi_d} & |\hat{t}-t_0-\kappa_w mT| < T_p \\ 0 & else \end{cases} \quad (18)$$

is the ambiguity function of a single sub-waveform, and in accordance with the hypothesis aforementioned, we have:

$$sac(m,\hat{t}) \approx sac(\hat{t}) = \begin{cases} \dfrac{2\sin((\mu(\hat{t}-t_0)+2\pi\xi_d)\frac{T_p-|\hat{t}-t_0|}{2})}{\mu(\hat{t}-t_0)+2\pi\xi_d} & |\hat{t}-t_0| < T_p \\ 0 & else \end{cases} \quad (19)$$

Substitute (17) and (19) into (16), and record:

$$\Delta\varphi_t = \varphi_{t_0} - \varphi_t \quad (20)$$

$$\Phi = \pi f_\Delta(\kappa+1)\hat{t} - \pi f_\Delta(\kappa+1)t_0 + \pi f_\Delta(2\kappa+\kappa_v\kappa_w)mT + \pi f_\Delta\kappa_v T_p + \Delta\varphi_t \quad (21)$$

$$C(m,\Delta\varphi_t,\hat{t}) = \sum_{k=0}^{K-1} e^{jk\Phi} = e^{j\frac{K-1}{2}\Phi} \cdot \frac{\sin(K\Phi/2)}{\sin(\Phi/2)} \quad (22)$$

$u_c(m,\hat{t})$ can be further expressed as:

$$u_c(m,\hat{t}) \approx \eta_0 e^{-j2\pi f_c\kappa t_0} e^{j2\pi f_c\kappa_v mT} e^{j\frac{\mu}{2}(\hat{t}-t_0-\kappa_w mT)T_p} \cdot e^{j\pi f_c\kappa_v(\hat{t}+t_0+\kappa_w mT+T_p)} \cdot sac(\hat{t}) \cdot C(m,\Delta\varphi_t,\hat{t}) \quad (23)$$

Take the modulus of $u_c(m,\hat{t})$ to analyze the amplitude character, then

$$|u_c(m,\hat{t})| = \eta_0 \cdot |sac(\hat{t})| \cdot |C(m,\Delta\varphi_t,\hat{t})| \quad (24)$$

It is indicated that the amplitude profile of the synthetical signal in a single period is determined by $|sac(\hat{t})|$ and $|C(m,\Delta\varphi_t,\hat{t})|$ (hereafter abbreviated as $|C|$ if needed). When m and $\Delta\varphi_t$ are determinate, $|C|$ can be regard as a discrete sinc function.

Fig.3 shows the relations among the matched output $|sac(\hat{t})|$, the discrete sinc function $|C|$ and the synthetical output $|u_c(m,\hat{t})|$. The main conditions for the simulation are: number of transmitting channels $K=16$, carrier frequency $f_c = 2GHz$, pulse repetition period $T = 1ms$, pulse width $T_p = 20\mu s$, chirp rate $\mu = 2\times10^{10}$, frequency interval $f_\Delta = 0.4MHz$, target velocity $v = 0\ m/s$, the target distance is $30\ km$, the sampling frequency is $20\ MHz$, the space phase difference corresponding to the target direction is $\varphi_t = \pi/2$, and assume the direction of the equivalent transmitting beam coincides with the target direction $\varphi_{t_0} = \pi/2$, namely $\Delta\varphi_t = 0$.

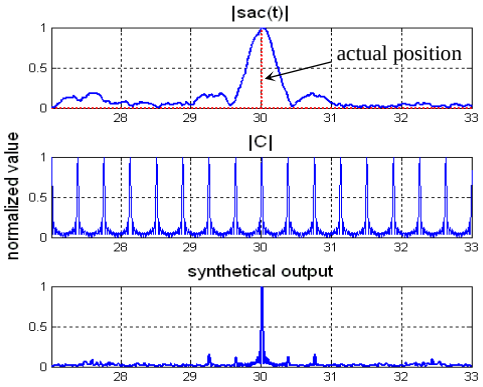

Fig.3 Relations among $|sac(\hat{t})|$, $|C|$ and the synthetical output $|u_c(m,\hat{t})|$.
($\varphi_{t_0}=\varphi_t=\pi/2$, $\Delta\varphi_t=0$)

The characteristic of the synthetical signal along with the range-direction coupling relationship mentioned in the following section have been discussed in detail in reference [16]. And reference [17] also has some correlative analysis. For more details, refer to.

4 Main factors affecting envelope migration

4.1 Range-direction coupling character of $|C|$

According to (21) and (22), let $\Phi=2n_m\pi$ (n_m is an arbitrary integer), and then the peak value point of $|C|$ can be obtained:

$$\hat{t}_m=t_0+\frac{2n_m}{(\kappa+1)f_\Delta}-\frac{(2\kappa+\kappa_v\kappa_w)mT}{\kappa+1}-\frac{\kappa_v T_p}{\kappa+1}-\frac{\Delta\varphi_t}{(\kappa+1)\pi f_\Delta} \quad (25)$$

Take notice of:

$$\left|C(m,\Delta\varphi_t+\psi,\hat{t})\right|=\left|C\left(m,\Delta\varphi_t,\hat{t}-\psi/((\kappa+1)\pi f_\Delta)\right)\right| \quad (26)$$

That is to say, a change of $\Delta\varphi_t$ will induce the migration of $|C|$ on the time-axis. $\Delta\varphi_t$ depends on the direction of equivalent transmitting beam. It is shown that there exists "range-direction coupling relationship" in item $|C|$. From formula (25), it also can be seen that due to the existence of item $\Delta\varphi_t/[(\kappa+1)\pi f_\Delta]$, $\hat{t}_m$ will change with of $\Delta\varphi_t$ when other parameters such as m and the target velocity are determinate.

Considering the periodicity of $|C|$, the synthetical signal $|u_c(m,\hat{t})|$ also has such coupling relationship. The simulation result in Fig.4 illustrates the coupling character of the synthetical signal. The conditions are the same to those of Fig.3 except that $\Delta\varphi_t=0$ is changed to $\Delta\varphi_t=\pi/2$. It can be seen that, even if the direction of equivalent transmitting beam deviates from the actual direction of the target, there is a good peak value output in the synthetical signal, only existing some deflection of the distance.

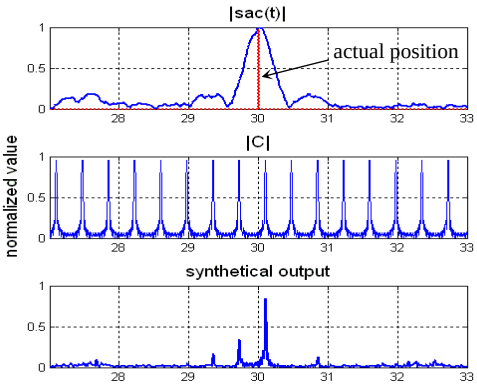

Fig.4 Relationship among $|sac(\hat{t})|$, $|C|$ and the synthetical output $|u_c(m,\hat{t})|$.
($\varphi_t=\pi/2$, $\varphi_{t_0}=0$, $\Delta\varphi_t=\pi/2$)

In the follows, we'll analyze the changing regularity of the synthetical signal envelope between pulse periods (PRIs) by studying the variety of the peak value of $|C|$ proceeding with formula (25). Make a passing mention that, due to the existence of item $\kappa_v T_p/(1+\kappa)$, the peak value points will deviate from the proper position slightly when the target velocity is not zero, but it is independent of the envelope migration between PRIs, so we don't care about it.

4.2 Range migration of static targets

For a static target, $\kappa=1$, $\kappa_v=\kappa_w=0$. We have:

$$\hat{t}_m = t_0 + \frac{n_m}{f_\Delta} - mT - \frac{\Delta\varphi_t}{2\pi f_\Delta} \quad (27)$$

It can be seen that, if $m = 0$ and $\Delta\varphi_t = 0$, one of the peak value points must be $\hat{t}_m = t_0$. However, it is not sure that there is a peak value point at t_0 when m increases (For example, when $f_\Delta T$ is not an integer). That is to say, the envelope of the synthetical signal of static target may move between different PRIs.

Since the discrete sinc function $|C|$ determines the accurate position of the mainlobe of synthetical signal, the peak value points of $|C|$ in different periods must be identical to ensure the identical alignment of the mainlobes in different periods. From formula (27), we can find the necessary and sufficient condition to guarantee no range migration for static target is:

$$n_{m+1} - n_m = n_\Delta = f_\Delta T \quad (28)$$

Here, n_Δ is a proper positive integer and is independent of the slow time m.

4.3 Range migration of moving targets

For a moving target, suppose the condition expressed by (28) is satisfied and the envelope migration of the synthetical signal during the whole integration time (namely CPI) doesn't exceed one period of the discrete sinc function. Similar with the situation of static target, we can get:

$$\hat{n}_m = mn_\Delta + n_0 \quad (29)$$

Here, $\hat{n}_m$ denotes the period sequence number of the peak value point of $|C|$ which determines the position of the mainlobe of the synthetical signal. n_0 is an integer which is concerned with the target distance and the receiving data sampling but independent of m.

Substitute (29) into (25), a simplified expression of $\hat{t}_m$ can be obtained: (Proof is referred to appendix)

$$\hat{t}_m = t_0 + \frac{2n_0T}{(1+\kappa)n_\Delta} - \frac{\kappa_v mT}{\kappa} - \frac{\kappa_v T_p}{\kappa+1} - \frac{\Delta\varphi_t}{(\kappa+1)\pi f_\Delta} \quad (30)$$

According to (30), it can be seen that, due to the existence of item $\kappa_v mT/\kappa$, the mainlobe of the synthetical signal will move regularly along with the pulse period. The mainlobe migration is exactly the range migration of moving target. So $\kappa_v mT/\kappa$ can be called as the range migration item, and κ_v/κ is defined as the range migration factor, which means the relative amount of migration between adjacent PRIs.

5 Range migration compensation method based on direction controlling

Range migration between pulse periods will result in the loss of coherent integration, and a compensation method based on direction controlling will be introduced in this section.

Through the foregoing analysis, it is indicated that the change of the direction of equivalent transmitting beam will induce the envelope migration of synthetical signal on time axis. Therefore, we can utilize this range-direction coupling character to compensate the range migration by adopting different rectifying phase difference φ_{t_0} in different period.

Here, phase difference φ_{t_0} is a function of period m, and it can be rewritten as $\varphi'_{t_0}(m)$, then

$$\varphi'_{t_0}(m) = \varphi_{t_0} - m\phi_\Delta \quad (31)$$

where ϕ_Δ is an increment of the rectifying phase difference between adjacent pulse periods for compensating the range migration, and can be called as direction modifying factor.

Similar with the forementioned directional deflection $\Delta\varphi_t$, we can define $\Delta\varphi'_t(m)$ as:

$$\Delta\varphi'_t(m) = \varphi'_{t_0}(m) - \varphi_t = \Delta\varphi_t - m\phi_\Delta \quad (32)$$

Substitute $\Delta\varphi'_t(m)$ for $\Delta\varphi_t$ in formula (30), the peak value point in compensation state can be got:

$$\hat{t}_c = t_0 + \frac{2n_0T}{(1+\kappa)n_\Delta} - \frac{\kappa_v mT}{\kappa} - \frac{\kappa_v T_p}{\kappa+1} - \frac{\Delta\varphi_t - m\phi_\Delta}{(\kappa+1)\pi f_\Delta} \quad (33)$$

In order to compensate the envelope migration across PRIs, $\hat{t}_c$ must be independent of m, so

$$\frac{\kappa_v mT}{\kappa} - \frac{m\phi_\Delta}{\pi(1+\kappa) f_\Delta} = 0 \quad (34)$$

and then

$$\phi_\Delta = \pi\kappa_v(1+\kappa)Tf_\Delta / \kappa \quad (35)$$

Therefore, the compensated synthetical signal can be approximately expressed as:

$$\begin{aligned} u_c'(m,\hat{t}) &\approx \sum_{k=0}^{K-1} y_{k,k}(m,\hat{t}) e^{jk\varphi_{t_0}'(m)} \\ &= \sum_{k=0}^{K-1} y_{k,k}(m,\hat{t}) e^{-jkm\phi_\Delta} e^{jk\varphi_{t_0}} \end{aligned} \quad (36)$$

According to formula (36), the compensation method can be described as follows: After down-conversion and matched filtering, K path of outputs are obtained for each pulse repetition period. In the m -th ($m = 0,1,\cdots,M-1$) period, multiply the matched filtering outputs by different circumrotation factors $e^{-jkm\phi_\Delta}$ ($k = 0,1,\cdots,K-1$). Then, synthesize the outputs through ordinary beamforming for each period. At last, the obtained synthetical signals in different periods can be integrated coherently. The whole processing scheme is illustrated in Fig.5.

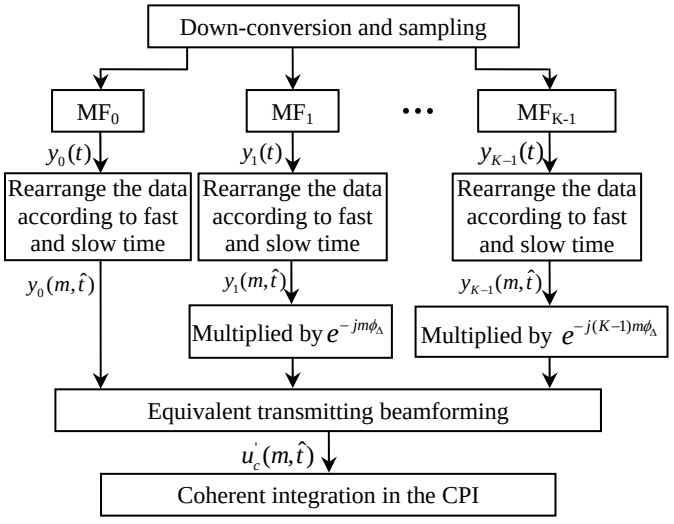

Fig.5 Range migration compensation scheme based on direction controlling

In practice, the steering vectors of equivalent transmitting beamforming required in each period can be calculated beforehand according to formula (31), (35) and (36). After receiving the returned signal, range migration compensation and signal synthesizing (namely beamforming) can be done simultaneously, so additional real-time computation burden will be reduced greatly.

There also exists some side effect in this compensation method. A direct influence is the generation of velocity estimation deflection. According to foregoing analysis, we can find that the Doppler frequency deflection resulting from the compensation is approximately:

$$\Delta f_d = \frac{\kappa_v}{2} B_\Sigma \quad (37)$$

where B_Σ is the total bandwidth of the system:

$$B_\Sigma = \mu T_p + (K-1) f_\Delta \quad (38)$$

In addition, it can be seen from formula (33) the phenomenon of range-direction coupling induced by $\Delta\varphi_t$ still exists. For a certain velocity, the corresponding ϕ_Δ is changeless, and it will compensate the range migration between PRIs exactly. The deflection of the peak value point caused by the range-direction coupling is fixed for each PRI, and it will not result in additional range migration.

6 Simulation results

The following figures show the effectiveness of the proposed compensation scheme. The main simulation conditions are: $K = 16$, $T = 1ms$, $T_p = 40\mu s$, $\mu = 1.25\times10^{10}$, $f_\Delta = 0.4MHz$, the target velocity is $v = 680\ s/m$, the target distance is $30\ km$, the space phase difference corresponding to the target direction is $\varphi_t = \pi/2$, and assume the direction of the equivalent transmitting beam coincides with the target direction $\varphi_{t_0} = \pi/2$, namely $\Delta\varphi_t = 0$.

Here, the condition expressed by (28) is satisfied. Therefore, the range migration across PRIs completely results from target motion. Fig.6 illustrates the instance of envelope migration. It can

be seen that, the peak value of the synthetical output in the last period deviates from that in the first period. It will produce much loss to integrate these synthetical signals of all periods directly, which is shown in Fig.7.

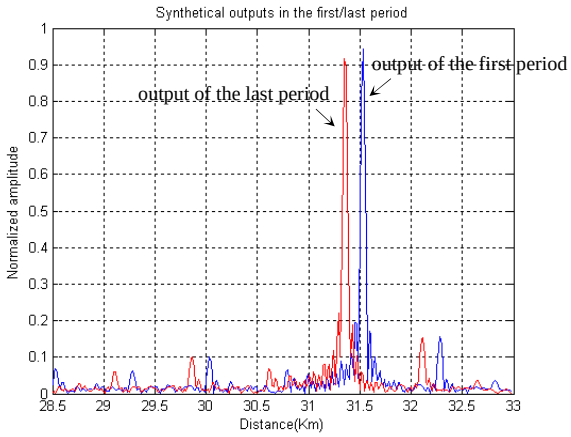

Fig.6 The envelope migration of the synthetical output without compensation

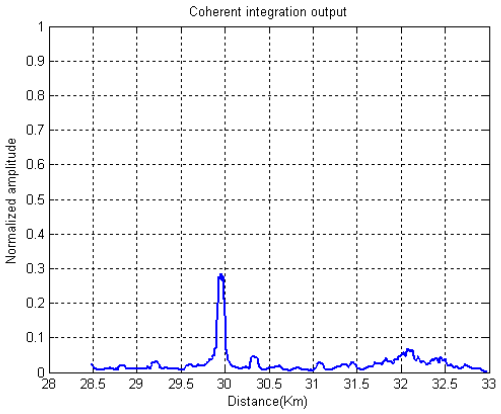

Fig.7 The coherent integration output without compensation ($\Delta\varphi_t = 0$)

Fig.8 shows the coherent integration output with compensation by the method proposed in this paper. The integration effect is improved remarkably.

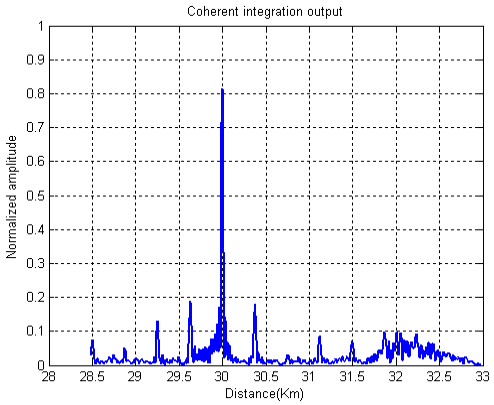

Fig.8 The coherent integration output with compensation ($\Delta\varphi_t = 0$)

When the phase difference of transmitting beamforming is changed from $\varphi_{t_0} = \pi/2$ to $\varphi_{t_0} = -\pi/2$, the result will be as shown in Fig.9 It can be seen that, though the direction of equivalent transmitting beam deviates from the actual target direction, good integration effect can be obtained except for a deflection in distance. This is the range-direction coupling phenomenon of the SFDLFM synthetical signal.

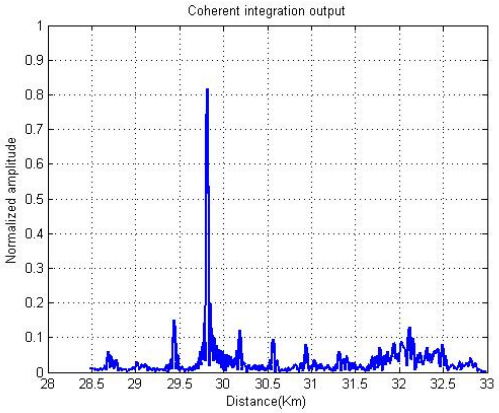

Fig.9 The coherent integration output with compensation ($\Delta\varphi_t = \pi$)

7 Conclusion

To offset the loss resulting from the low-gain transmitting beam in orthogonal signal MIMO radar, long integration time must be required. For long time coherent integration, a vital problem is to resolve the range migration of moving targets. The range migration compensation problem with known apriori information about the target velocity in

SFDLFM-MIMO radar is discussed, and a compensation method utilizing the range-direction coupling relationship of the synthetical output of SFDLFM signal is proposed in this paper. In this method the compensation operation is combined with the processing of signal synthesizing. Almost no additional computation burden is introduced since the synthesizing processing is the inherent operation in MIMO radar. The proposed method is much suitable to MIMO radar when searching for ordinary aerodynamic targets.

It can be seen from the simulation results that there exist considerable sidelobes in the synthetical output, which will influence the detection and tracking capabilities of the radar. These sidelobes can be controlled by some restraining techniques and certain processing aimed at sub-band signal. For lack of space, expert discussion is not carried out in this paper, and it will be presented in the following paper.

References:

[1] D. J. Rabideau, P. Parker, Ubiquitous MIMO multifunction digital array radar, *Conference Record of the 37th Asilomar Conference on Signals, Systems and Computers*, Vol. 1, Nov. 2003, pp. 1057-1064.

[2] F. C. Robey, S. Coutts, Weikle D C, et al. MIMO radar theory and experimental results, *Conference Record of the 38th Asilomar Conference on Signals, Systems and Computers*, Vol.1, 2004, pp. 300-304.

[3] Tabrikian J. Barankin, Bounds for Target Localization by MIMO Radars, *4th IEEE Workshop on Sensor Array and Multichannel Processing*, Vol.1, 2006, pp. 278-281.

[4] Bekkerman I, Tabrikian J, Target detection and localization using MIMO radars and sonars, *IEEE Trans. on Signal Processing*, Vol.54, No. 10, 2006, pp. 3873-3883.

[5] C. C. Chen, H. C. Andrews, Targets motion induced radar imaging, *IEEE Trans on Aerosp. Electron. Syst.*, vol.16, no.1, Jan. 1980, pp. 2–14.

[6] G. Y. Delisle, H. Wu, Moving target imaging and trajectory computation using ISAR. *IEEE Trans. Aerosp. Electron. Syst*., vol.30, no.3, 1994, pp. 887–899.

[7] Y. Z. Chen, Y. F. Zhu, H. Z. Zhao, Q. Fu, Detection algorithm research of high velocity moving target based on the envelope interpolation, *Signal processing (China)*, vol.20, no.4, Aug. 2004, pp.387-390.

[8] J. Wang, S. H. Zhang; Z. Bao, On motion compensation for weak radar reflected signal detection, *6th International Conference on Signal Processing*, vol.2, 2002, pp. 1445 – 1448.

[9] R. P. Perry, R C. Dipietro, R. L. Fante, SAR Imaging of Moving Targets, *IEEE Trans on Aerosp. Electron. Syst*., vol.35, no.1, Jan. 1999, pp,188 – 200.

[10] R. P. perry, R C. Dipietro, R. L. Fante, Coherent Integration With Range Migration Using Keystone Formatting, *Radar Conference, 2007 IEEE*, Apr. 2007, pp.863 – 868.

[11] Luce A, Experimental results on SIAR digital beamforming radar, *Proc. of the IEEE International Radar Conference*, Vol.1, 1992, pp.505-510.

[12] Dorey J, Garnier G, Auvray G.RIAS, Synthetic Impulse and Antenna Radar, *1989 International Conference on Radar*,Vol.1, 1989, pp.556-562.

[13] Q. W. Zhang, Z. Bao, Y. H. Zhang, Time-Space 3-D Matched Filtering and Performance Analysis of SIAR, *Journal of Electronics (China)*, Vol.16, No. 5, 1994, pp.481-489.

[14] B. X. Chen, H. L. Liu, S. H. Zhang, Long-time coherent integration based on sparse-array synthetic impulse and aperture radar, *Proceedings of CIE International Conference on Radar*, Oct. 2001, pp.1062 – 1066.

[15] X. Z. Dai, J. Xu, C. M. Ye, Y. N. Peng, Low-sidelobe HRR profiling based on the FDLFM-MIMO radar Synthetic Aperture Radar, *APSAR 2007. 1st Asian and Pacific Conference on*, 5-9 Nov. 2007, pp.132 – 135.

[16] H. M. Liu, Z. S. He, T. Chen, J. Li, S. H. Hu, Analysis on characteristics of MIMO Radar with stepped frequency division linear frequency modulation signal, submitted to the *IEEE Journal of Selected Topics in Signal Processing* 2009.

[17] X. Z. Dai, J. Xu, Y. N. Peng, High Resolution Frequency MIMO Radar, *IEEE Radar Conference*, Apr. 2007, pp. 693 – 698.

[18] Y. B. Zhao, M. C. Liu, S. H. Zhang, The Grating Lobe Induced by the Coupling of Range and Direction in SIAR and Its Elimination. *Journal of Electronics and Information Technology (China)*, Vol.23, No. 4, 2001, pp.360-364.

[19] L. F. Ding, F. L. Geng, *Radar principle (third edition)*, 2002, Xi'an (China): Xidian University publishing house

[20] B. Liu, C. L. Han, B. Y. Liu. Receiving Signal Processing of Wideband MIMO Radar Based

On Transmitting Diversity, *CIE International Conference on Radar*, Vol. 1, Oct. 2006, pp. 20-23.

Appendix

Proof of formalu (30):

$\because \quad \hat{n}_m = mn_\Delta + n_0$ and $n_{m+1} - n_m = n_\Delta = f_\Delta T$

$$\therefore \quad \frac{2\hat{n}_m}{(1+\kappa) f_\Delta} = \frac{2n_m T}{(1+\kappa)n_\Delta} = \frac{2m\hat{n}_\Delta T}{(1+\kappa)n_\Delta} + \frac{2n_0 T}{(1+\kappa)n_\Delta}$$
$$= \frac{2mT}{(1+\kappa)} + \frac{2n_0 T}{(1+\kappa)n_\Delta}$$

and,

$$\because \quad \frac{(2\kappa_v + \kappa_v\kappa_w)}{\kappa+1} = \frac{\kappa_v(2+\kappa_w)}{\kappa+1} = \frac{\kappa_v(1/\kappa+1)}{\kappa+1}$$

$$= \frac{\kappa_v(1+\kappa)}{\kappa(\kappa+1)} = \frac{\kappa_v}{\kappa}$$

$$\therefore \quad \frac{(2\kappa+\kappa_v\kappa_w)mT}{\kappa+1} = \frac{(2+2\kappa_v+\kappa_v\kappa_w)mT}{\kappa+1}$$

$$= \frac{2mT}{\kappa+1} + \frac{(2\kappa_v+\kappa_v\kappa_w)mT}{\kappa+1} = \frac{2mT}{\kappa+1} + \frac{\kappa_v mT}{\kappa}$$

so,

$$\hat{t}_m = t_0 + \frac{2\hat{n}_m}{(\kappa+1) f_\Delta} - \frac{(2\kappa+\kappa_v\kappa_w)mT}{\kappa+1}$$
$$- \frac{\kappa_v T_p}{\kappa+1} - \frac{\Delta\varphi_t}{(\kappa+1)\pi f_\Delta}$$
$$= t_0 + \left(\frac{2mT}{(1+\kappa)} + \frac{2n_0 T}{(1+\kappa)n_\Delta} \right)$$
$$- \left(\frac{2mT}{\kappa+1} + \frac{\kappa_v mT}{\kappa} \right) - \frac{\kappa_v T_p}{\kappa+1} - \frac{\Delta\varphi_t}{(\kappa+1)\pi f_\Delta}$$
$$= t_0 + \frac{2n_0 T}{(1+\kappa)n_\Delta} - \frac{\kappa_v}{\kappa} mT - \frac{\kappa_v T_p}{\kappa+1} - \frac{\Delta\varphi_t}{(\kappa+1)\pi f_\Delta}$$